DOI: 10.1002/ejic.201100170

A Metallocorrole with Orthogonal Pyrrole Rings

Kolle E. Thomas,[a] Jeanet Conradie,[b] Lars K. Hansen,[a] and Abhik Ghosh*[a]

Keywords: Aromaticity / Chirality / Corroles / Trifluoromethylated compounds

In contrast to sterically hindered metalloporphyrins, which are almost always strongly nonplanar, similarly substituted metallocorroles are generally relatively planar. A crystal structure of a copper β-octakis(trifluoromethyl)-*meso*-triarylcorrole, however, has revealed a corrole macrocycle with an unprecedented degree of saddling. With the exception of the bipyrrole unit, any two adjacent pyrrole rings are essentially orthogonal to each other. Furthermore, the C_2-symmetric molecular structure is chiral and NMR spectroscopy and DFT calculations suggest that the enantiomers do not interconvert readily. Once resolved, the molecule may provide us with a novel example of an inherently chiral chromophore.

Introduction

As we head into the twenty-first century, novel aromatics continue to capture the imagination of chemists. Aromaticity is not only a fascinating electronic–structural phenomenon, responsible for a variety of spectroscopic properties such as intense one- and two-photon absorption,[1,2] aromatics, by virtue of their stability, lend themselves to a host of technological applications, such as photovoltaics,[3] liquid crystals,[4] biological imaging agents,[5] and two-photon absorbers.[2] Nonplanar[6] and chiral[7] aromatics, on account of their topologies, are a particularly intriguing class of molecules, notable not only for their optical/chiroptical properties but also as tools for molecular/chiral recognition.[8] The study of porphyrins and related macrocycles has contributed greatly to our appreciation of aromaticity, as it has to many other fields of modern chemistry. While ruffled and saddled porphyrins have long been known,[9] recent notable contributions to the subject include a number of conical subporphyrin derivatives[10] and figure-eight-like expanded porphyrins;[11] the latter compounds provide rare and fascinating examples of Möbius aromaticity.[12,13] Against this context, we recently found that copper corroles are inherently saddled and that the saddling may be amplified by sterically hindered peripheral substituents;[14,15] these molecules are thus unique examples of nonplanar, chiral and C_2-symmetric porphyrin-type aromatics. The most sterically hindered copper corroles that we have synthesized are a class of copper β-octakis(trifluoromethyl)-*meso*-triarylcorroles with varying *para*-substituents on the *meso*-aryl

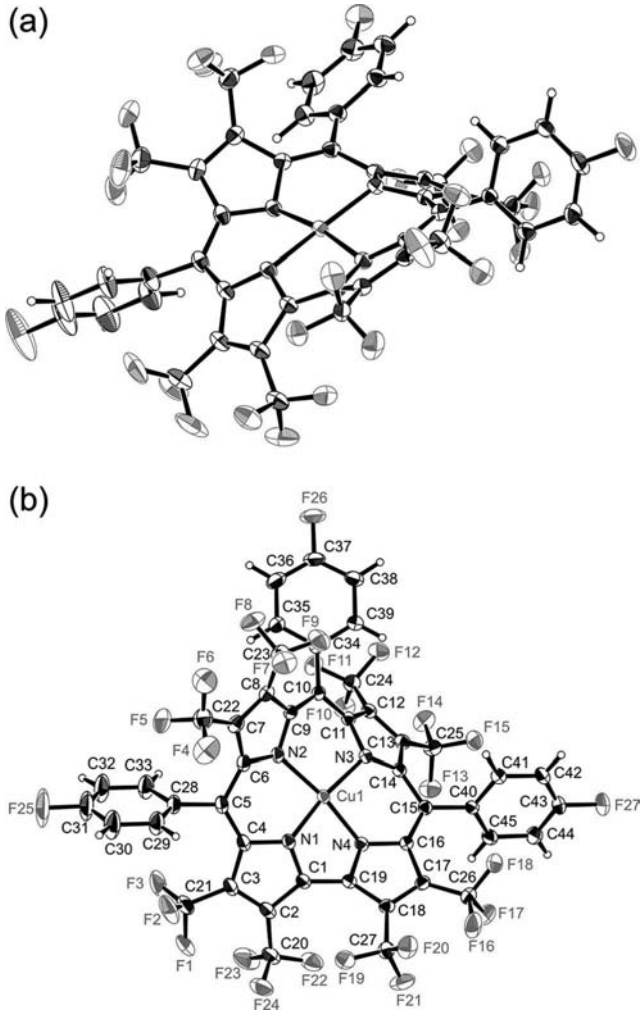

Figure 1. Two ORTEP views of **1**. Distances [Å]: Cu–N1 1.929(3), Cu–N2 1.922(4), Cu–N3 1.927(3), Cu–N4 1.914(4); dihedrals [°]: C3–C4–C6–C7 83.2, C8–C10–C11-C12 84.5, C13–C14–C16–C17 89.6, C2–C1–C19–C18 57.2.

[a] Department of Chemistry and Center for Theoretical and Computational Chemistry, University of Tromsø
9037 Tromsø, Norway
Fax: +47-77644765
E-mail: abhik.ghosh@uit.no
[b] Department of Chemistry, University of the Free State
9300 Bloemfontein, Republic of South Africa

Supporting information for this article is available on the WWW under http://dx.doi.org/10.1002/ejic.201100170.

groups, Cu[$(CF_3)_8$T(*p*-X-P)C].[16] These complexes exhibit very high reduction potentials and exceedingly strong *meso* substituent effects on the position of the Soret maximum. Unfortunately, none of these complexes has lent itself to an X-ray structure determination. Indeed their inaccessibility and scarceness has discouraged detailed physical measurements on these fascinating molecules. Careful repetition of the syntheses, however, established that the *p*-fluorophenyl complex, Cu[$(CF_3)_8$T(*p*-F-P)C] (**1**), could be synthesized with relative ease and in larger quantities, allowing us to ultimately determine its structure by single-crystal X-ray diffraction, as shown in Figure 1 and described below.

Results and Discussion

Complex **1** is by far the most strongly saddled structure for any metallocorrole.[17,18] Except for the C1–C19 bipyrrole linkage, any two adjacent pyrrole rings are nearly orthogonal to each other. This may be verified from the "saddling dihedrals" listed above (see Figure 1 caption). The structure is also notable for multiple F···F nonbonded contacts that are shorter than two times the van der Waals radius of fluorine. Yet a third but related unusual feature is that none of the eight CF_3 groups exhibits rotational disorder, which is very common for trifluoromethylated compounds; once again, this feature is readily attributed to the sterically hindered nature of the molecule.

It is important to emphasize that the unprecedented nonplanar geometry of **1** reflects a combination of electronic and steric effects. Saddling is driven in the first place by the tendency of the electrons in the corrole π-HOMO to flow into the formally empty $d_{x^2-y^2}$ orbital of the "Cu^{III}" center; in other words, the complex is best viewed as Cu^{II}-corrole$^{\cdot 2-}$.[14,15] In the absence of such noninnocence,[19] corroles are remarkably resistant to saddling. Thus, unlike copper β-octabromo-*meso*-triarylcorroles, the analogous group 9 (Co, Rh, Ir) complexes all feature *planar* corrole cores.[20] Such planarity may again be contrasted with a host of β-octabromo-*meso*-tetraarylmetalloporphyrin structures,[9] which, without exception, are saddled. In view of the general preference of the corroles for planar structures, the fact that **1** is actually considerably more saddled than a structurally characterized, formally isoelectronic Ni^{II} β-octakis(trifluoromethyl)-*meso*-tetraarylporphyrin derivative is remarkable.[21] Geometry optimizations with dispersion-corrected density functional theory (DFT,[22] BP86[23]-D[24]/STO-TZP) nicely reproduce all of the above structural features (see Figure 2), most notably the saddling dihedrals. Without the dispersion corrections, DFT (BP86/TZP) does less well and overestimates the saddling dihedrals by 10–15° relative to BP86-D.

Variable-temperature ^{1}H and ^{19}F NMR measurements from +100 to –80 °C (the temperature range available to us) provided insight into the dynamic behavior of **1**. In general, there is considerably less overlap between ^{1}H NMR peaks at –80 °C than at room temperature (Figure 3a). Despite partial overlap between two sets of peaks (A and B; D and E, Figure 3b), the ^{1}H NMR spectrum at –80 °C shows clear evidence of six equal-sized peaks, exactly as expected on the basis of a strongly saddled structure with time-averaged C_2 symmetry. Each proton on each of the 5,15-aryl groups is symmetry distinct, although because the two aryl groups are related by a molecular C_2 axis, each of these protons occurs as a set of two. For the 10-aryl group, the two *ortho* protons are homotopic, as are the two *meta* protons. This peak pattern rules out the occurrence of saddling inversion on the NMR timescale.

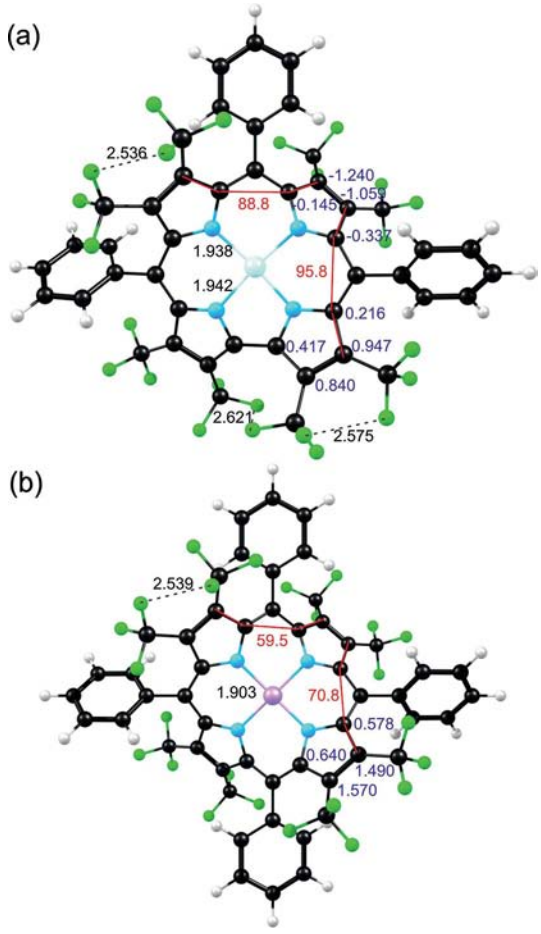

Figure 2. BP86-D optimized geometries of (a) Cu[$(CF_3)_8$TPC] and (b) Ni[$(CF_3)_8$TPP]. Interatomic distances (in black) and out-of-plane distances (in blue) are in Å; dihedrals are in °.

As noted before,[16] the CF_3 fluorine atoms appear as quartets with high $^5J_{FF}$ coupling constants (≈10–15 Hz) in the ^{19}F NMR spectra at room temperature and above. This was interpreted as reflecting fast rotation (on the NMR timescale) of the congested, but dynamically geared CF_3 groups; thus, each CF_3 fluorine is only split by the three fluorines on the neighboring CF_3 group. As the temperature is lowered, two of the ^{19}F CF_3 peaks (R and Q in Figure 3c), which are partially overlapped at room temperature, move apart. In addition, the CF_3 peaks all broaden considerably at –80 °C relative to those at room temperature. Although instrumental limitations prevented us from going to even lower temperatures, we are tempted to speculate

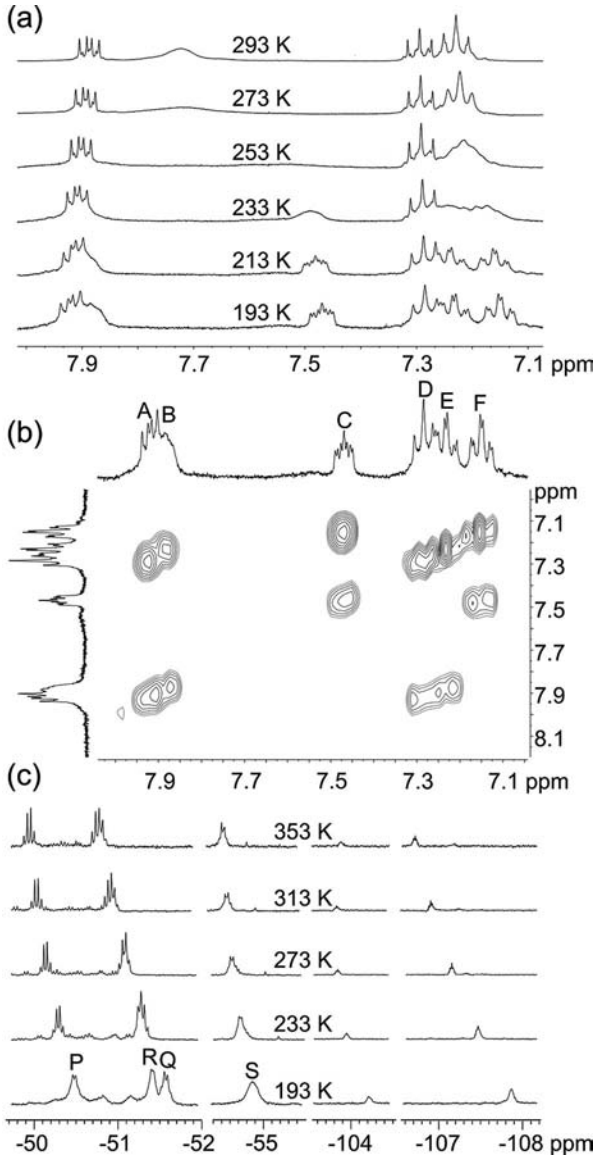

Figure 3. Variable-temperature (a) ^{1}H NMR and (b) ^{1}H-^{1}H COSY of **1** in CD_2Cl_2; (c) ^{19}F NMR in [D_8]toluene.

that the broadening reflects the onset of intra-CF_3 ^{19}F-^{19}F coupling as a result of slowing CF_3 rotation on the NMR timescale.

We next sought to shed light, using DFT calculations, on some of the unique physical properties of Cu[$(CF_3)_8$T(*p*-X-P)C] derivatives that we have alluded to above. Above all, we wished to obtain and, gratifyingly, succeeded in obtaining a clear, qualitative explanation for the very large *meso*-substituent effects on the Soret maxima of Cu[$(CF_3)_8$-T(*p*-X-P)C] corroles. Thus, between X = H and X = OCH_3, the Soret maximum of Cu[$(CF_3)_8$T(*p*-X-P)C] is redshifted by 48 nm.[16] The corresponding shifts are only 20 nm and 29 nm for the Cu[T(*p*-X-P)C] and Cu[Br_8T(*p*-X-P)C] series,[25] respectively. In our synthetic paper on the subject,[16] we suggested that the large *meso* shifts for the β-$(CF_3)_8$ complexes presumably reflect enhanced electronic communication between the corrole macrocycle and the aryl groups as a result of strong saddling. A more detailed TDDFT examination of the problem, however, indicates a different explanation.

Time-dependent BP86 calculations (Figure 4) do a fair job of reproducing the Soret redshifts along the series Cu[TPC] → Cu[Br_8TPC] → Cu[$(CF_3)_8$TPC]. Shifts in the

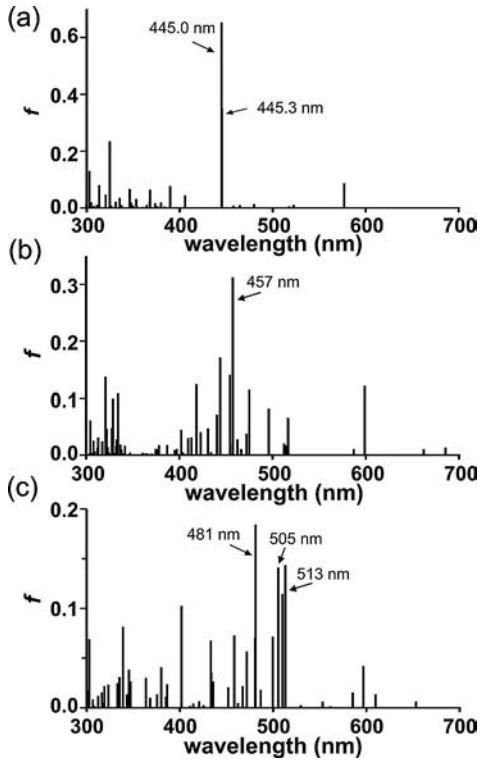

Figure 4. Artificial electronic absorption spectra of (a) Cu[TPC], (b) Cu[Br_8TPC], and (c) Cu[$(CF_3)_8$TPC], based on time-dependent BP86/STO-TZP calculations.

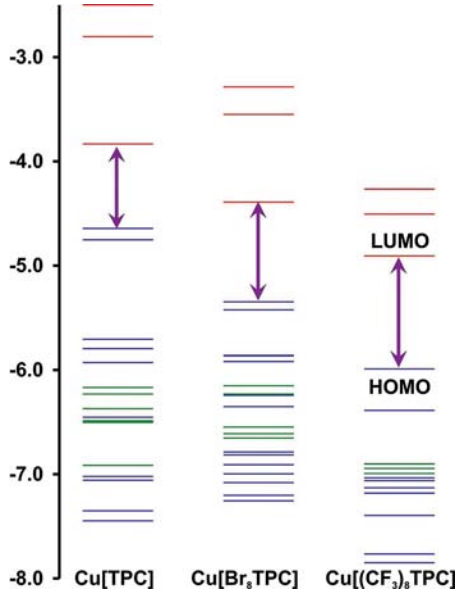

Figure 5. BP86-D Kohn–Sham MO energy levels [eV] for copper corroles. Unoccupied MO energy levels are indicated in red and occupied levels in blue or green; the green levels indicate MOs that are largely localized on the phenyl groups.

Kohn–Sham MO energy levels (Figure 5) are in qualitative accord with differences in electrochemical redox potentials. Explicit calculations of ionization potentials and electron affinities (Table S9), with and without solvent corrections, provide even greater insight, as detailed in the Supporting Information. Here, we wish to draw attention to the effect of the eight CF_3 groups on the corrole π orbital energies. As shown in Figures 5 and 6 (see Section 4, Supporting Information for detailed MO pictures), with the exception of the top two HOMOs, most of the higher-energy occupied MOs of Cu[$(CF_3)_8$TPC] are not corrole-based MOs but are *meso*-phenyl-based; the orbital energies of the majority of the occupied corrole π MOs have been greatly lowered by the eight electron-withdrawing CF_3 groups. Since copper corrole Soret bands have considerable phenyl-to-LUMO charge-transfer character,[25,26] it is understandable that such character should be even more pronounced for the β-$(CF_3)_8$ complexes. This is indeed the case, as shown in Table 1. The reader may verify that the main Soret transitions of Cu[$(CF_3)_8$TPC] have much greater aryl-to-Cu/corrole character than those of Cu[TPC] and Cu[Br_8TPC].

To conclude, we return to the subject of nonplanar aromatics and chirality. Complex **1** represents a new, chemically rugged, exceptionally nonplanar, aromatic chromophore, and by far the most strongly saddled metallocorrole reported to date. Although the above results represent a culmination of sorts of our recent studies on nonplanar deformations of corroles,[14,15] gratifyingly, they also mark the beginning of a new quest. The ^{1}H NMR studies mentioned above have established that the chiral, saddled structure of **1** does not enantiomerize on the NMR timescale. Although we have so far failed to locate a transition state for the

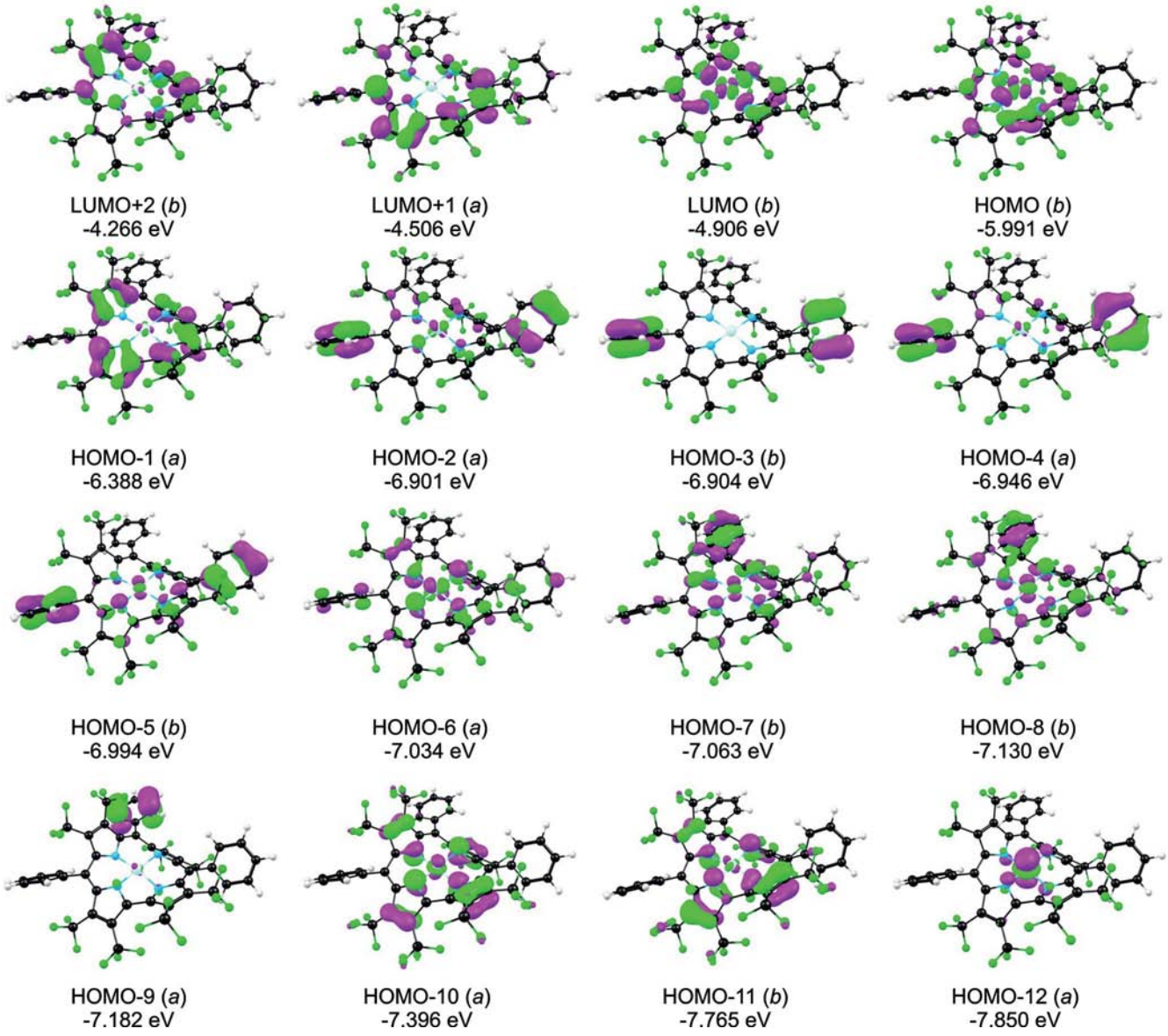

Figure 6. Kohn–Sham frontier MOs from BP86/STO-TZP calculations.

Table 1. Time-dependent BP86/STO-TZP results on the most intense Soret features of Cu[TPC], Cu[Br_8TPC], and Cu[$(CF_3)_8$TPC]: wavelengths (λ, nm) and oscillator strengths (f).

λ (nm)	Symmetry	f	From	To	%
Cu[TPC]					
445.0	B	0.653	HOMO-1	LUMO+2	54.3
			HOMO	LUMO+1	14.6
			HOMO-5	LUMO	11.5
			HOMO-15	LUMO	5.0
445.3	A	0.351	HOMO	LUMO+2	26.9
			HOMO-1	LUMO+1	24.3
			HOMO-6	LUMO	16.6
			HOMO-12	LUMO	8.6
			HOMO-2	LUMO+1	6.4
			HOMO-10	LUMO	5.0
Cu[Br_8TPC]					
457.4	B	0.312	HOMO-1	LUMO+2	19.4
			HOMO-13	LUMO	17.8
			HOMO-15	LUMO	13.4
			HOMO-2	LUMO+2	12.5
			HOMO-7	LUMO+1	10.9
			HOMO	LUMO+1	7.2
443.8	A	0.171	HOMO-6	LUMO+1	53.3
			HOMO-16	LUMO	10.9
			HOMO-14	LUMO	8.7
			HOMO	LUMO+2	8.3
			HOMO-18	LUMO	5.3
Cu[$(CF_3)_8$TPC]					
481	A	0.184	HOMO-4	LUMO+1	40.1
			HOMO-2	LUMO+1	17.9
			HOMO-6	LUMO+1	9.6
			HOMO-7	LUMO	7.3
			HOMO-1	LUMO+1	7.2
513	B	0.144	HOMO-3	LUMO+1	55.4
			HOMO-1	LUMO+2	29.8
			HOMO-2	LUMO	4.21
505	B	0.141	HOMO-3	LUMO+1	39.2
			HOMO-1	LUMO+2	34.3
			HOMO-5	LUMO+1	8.5

process, DFT calculations indicate a lower limit of 2.0 eV for the barrier to enantiomerization of Cu[$(CF_3)_8$TPC]. We thus look forward to synthesizing inherently chiral corrole-based chromophores in enatiomerically pure form within the foreseeable future and to studying their chiroptical properties and evaluating their potential as chiral recognition elements and as novel oriented materials.

Experimental Section

Complex **1**, Cu[$(CF_3)_8$T(*p*-F-P)C], was synthesized and purified as described previously.[16] A prefiltered, saturated dichloromethane solution of **1** (8 mg) in a glass vial was carefully layered with five times its volume of *n*-heptane. Slow evaporation of the solution from the undisturbed, open vial gave dark brown prismlike crystals within 10 d; these proved suitable for X-ray analysis.

All DFT calculations were carried out with the ADF 2009 program system,[27] by using STO-TZP basis sets, fine meshes for numerical integration of matrix elements, and tight geometry optimization criteria.

CCDC-815952 contains the supplementary crystallographic data for **1**. These data can be obtained free of charge from The Cambridge Crystallographic Data Centre via www.ccdc.cam.ac.uk/data_request/cif.

Supporting Information (see footnote on the first page of this article): Computational details are presented.

Acknowledgments

This work was supported by the Research Council of Norway and National Research Fund of South Africa.

[1] For a journal special issue on aromaticity, see: P. v. R. Schleyer, *Chem. Rev.* **2001**, *101*, 1115–1118.
[2] J. Y. Shin, K. S. Kim, M. C. Yoon, J. M. Lim, Z. S. Yoon, A. Osuka, D. Kim, *Chem. Soc. Rev.* **2010**, *39*, 2751–67.
[3] a) P. A. Troshin, R. Koeppe, D. K. Susarova, N. V. Polyakova, A. S. Peregudov, V. F. Razumov, N. S. Sariciftci, R. N. Lyubovskaya, *J. Mater. Chem.* **2009**, *19*, 7738–7744; b) F. G. Brunetti, X. Gong, M. Tong, A. J. Heeger, F. Wudl, *Angew. Chem.* **2010**, *122*, 542; *Angew. Chem. Int. Ed.* **2010**, *49*, 532–536.
[4] a) S. Sergeyev, W. Pisula, Y. H. Geerts, *Chem. Soc. Rev.* **2007**, *36*, 1902–1929; b) S. Laschat, A. Baro, N. Steinke, F. Giesselman, C. Hagele, G. Scalia, R. Judele, E. Kapatsina, S. Sauer, A. Schreivogel, M. Tosoni, *Angew. Chem.* **2007**, *119*, 4916; *Angew. Chem. Int. Ed.* **2007**, *46*, 4832–4887.
[5] S. Mathai, D. K. Bird, S. S. Stylli, T. A. Smth, K. P. Ghiggino, *Photochem. Photobiol. Sci.* **2007**, *6*, 1019–1026.
[6] M. Bühl, A. Hirsch, *Chem. Rev.* **2001**, *101*, 1153–1184.
[7] a) S. M. Rappaport, H. S. Rzepa, *J. Am. Chem. Soc.* **2008**, *130*, 7613–7619; b) A. Urbano, *Angew. Chem.* **2003**, *115*, 4116; *Angew. Chem. Int. Ed.* **2003**, *42*, 3986–3989; c) A. Rajca, M. Miyasaka in *Functional Organic Materials. Syntheses, Strategies, and Applications* (Eds.: J. J. Müller, U. H. F. Bunz), Wiley-VCH, Weinheim, **2007**, ch. 15, pp. 547–581; d) F. Diederich, R. L. Whetten, C. Thilgen, R. Ettl, I. Chao, M. M. Alvarez, *Science* **1991**, *254*, 1768–1770.
[8] a) C. Seel, F. Vogtle, *Angew. Chem.* **1992**, *104*, 542; *Angew. Chem. Int. Ed. Engl.* **1992**, *31*, 528–549; b) S. K. Narasimhan, D. J. Kerwood, L. Wu, J. Li, R. Lombardi, T. B. Freedman, Y. Y. Luk, *J. Org. Chem.* **2009**, *74*, 7023–7033.
[9] a) J. A. Shelnutt, X. Z. Song, J. G. Ma, S. L. Jia, W. Jentzen, C. J. Medforth, *Chem. Soc. Rev.* **1998**, *27*, 31–41; b) M. Senge, *Chem. Commun.* **2006**, 243–256.
[10] Y. Inokuma, A. Osuka, *Dalton Trans.* **2008**, 2517–2526.
[11] R. Mishra, T. K. Chandrashekar, *Acc. Chem. Res.* **2008**, *41*, 265–279.
[12] H. S. Rzepa, *Chem. Rev.* **2005**, *105*, 3697–3715.
[13] Z. S. Yoon, A. Osuka, D. Kim, *Nature Chem.* **2009**, *1*, 113–122.
[14] A. B. Alemayehu, E. Gonzalez, L.-K. Hansen, A. Ghosh, *Inorg. Chem.* **2009**, *48*, 7794–7799.
[15] A. B. Alemayehu, E. Gonzalez, L.-K. Hansen, A. Ghosh, *Inorg. Chem.* **2010**, *49*, 7608–7610.
[16] K. E. Thomas, I. H. Wasbotten, A. Ghosh, *Inorg. Chem.* **2008**, *47*, 10469–10478.
[17] Review on corroles: I. Aviv-Harel, Z. Gross, *Chem. Eur. J.* **2009**, *15*, 8382–8394.
[18] Examples of corrole saddling: a) C. Brückner, R. P. Brinas, J. A. K. Bauer, *Inorg. Chem.* **2003**, *42*, 4495–4497; b) I. Luobeznova, L. Simkhovich, I. Goldberg, Z. Gross, *Eur. J. Inorg. Chem.* **2004**, 1724–1732; c) M. Bröring, F. Bregier, E. C. Tejero, C. Hell, M. C. Holthausen, *Angew. Chem.* **2007**, *119*, 449; *Angew. Chem. Int. Ed.* **2007**, *46*, 445–448.
[19] a) F. A. Walker, S. Licoccia, R. Paolesse, *J. Inorg. Biochem.* **2006**, *100*, 810–837; b) B. O. Roos, V. Veryazov, J. Conradie, P. R. Taylor, A. Ghosh, *J. Phys. Chem. B* **2008**, *112*, 14099–14102.

[20] a) R. Paolesse, S. Nardis, F. Sagone, R. G. Khoury, *J. Org. Chem.* **2001**, *66*, 550–556; b) J. H. Palmer, M. W. Day, A. D. Wilson, L. M. Henling, Z. Gross, H. B. Gray, *J. Am. Chem. Soc.* **2008**, *130*, 7786–7787.
[21] C. Liu, Q.-Y. Chen, *Eur. J. Org. Chem.* **2005**, 3680–3686.
[22] DFT studies on corroles and corrole analogues: a) A. Ghosh, K. Jynge, *Chem. Eur. J.* **1997**, *3*, 823–833; b) A. Ghosh, T. Wondimagegn, A. B. J. Parusel, *J. Am. Chem. Soc.* **2000**, *122*, 5100–5104; c) J. Bendix, I. J. Dmochowski, H. B. Gray, A. Mahammed, L. Simkhovich, Z. Gross, *Angew. Chem.* **2000**, *112*, 4214; *Angew. Chem. Int. Ed.* **2000**, *39*, 4048–4051; d) E. Tangen, A. Ghosh, *J. Am. Chem. Soc.* **2002**, *124*, 8117–8121; e) B. van Oort, E. Tangen, A. Ghosh, *Eur. J. Inorg. Chem.* **2004**, 2442–2445; f) A. Ghosh, I. H. Wasbotten, W. Davis, J. C. Swarts, *Eur. J. Inorg. Chem.* **2005**, 4479–4485; g) I. H. Wasbotten, A. Ghosh, *Inorg. Chem.* **2006**, *45*, 4910–4913; h) A. M. Albrett, J. Conradie, A. Ghosh, P. J. Brothers, *Dalton Trans.* **2008**, 4464–4473.
[23] a) A. D. Becke, *Phys. Rev. A* **1988**, *38*, 3098–3100; b) J. P. Perdew, *Phys. Rev. B* **1986**, *33*, 8822; Erratum: J. P. Perdew, *Phys. Rev. B* **1986**, *34*, 7406.
[24] S. Grimme, *J. Comput. Chem.* **2006**, *27*, 1787–1799.
[25] I. H. Wasbotten, T. Wondimagegn, A. Ghosh, *J. Am. Chem. Soc.* **2002**, *124*, 8104–8116.
[26] A. Alemayehu, J. Conradie, A. Ghosh, *Eur. J. Inorg. Chem.* **2011**, 1857–1864; preceding paper.
[27] G. T. Velde, F. M. Bickelhaupt, E. J. Baerends, C. F. Guerra, S. J. A. van Gisbergen, J. G. Snijders, T. Ziegler, *J. Comput. Chem.* **2001**, *22*, 931–967.

Received: February 20, 2011
Published Online: March 16, 2011

